Received: 26 June 2020 | Accepted: 6 July 2020

DOI: 10.1002/jcc.26391

FULL PAPER

Journal of COMPUTATIONAL CHEMISTRY WILEY

On the strength of hydrogen bonding within water clusters on the coordination limit

Víctor Manuel Castor-Villegas[1] | José Manuel Guevara-Vela[1] | Wilmer E. Vallejo Narváez[2] | Ángel Martín Pendás[3] | Tomás Rocha-Rinza[1] | Alberto Fernández-Alarcón[1,4]

[1]Instituto de Química, Universidad Nacional Autónoma de México, Circuito Exterior, Ciudad Universitaria, Mexico City, Mexico

[2]Institute of Materials Research, National Autonomous University of Mexico, Circuito Exterior, Ciudad Universitaria, Mexico City, Mexico

[3]Department of Analytical and Physical Chemistry, University of Oviedo, Oviedo, Spain

[4]Universidad Iberoamericana, Prolongacion Paseo de Reforma 880, Mexico City, Mexico

Correspondence
Tomás Rocha-Rinza and Alberto Fernández-Alarcón, Institute of Chemistry, National Autonomous University of Mexico, Circuito Exterior, Ciudad Universitaria, Delegación Coyoacán C.P. 04510, Mexico City, Mexico.
Email: trocha@iquimica.unam.mx (T. R.-R.);
Email: al.fedza@gmail.com (A. F.-A.)

Funding information
Consejo Nacional de Ciencia y Tecnología, Grant/Award Number: 253776; DGTIC/UNAM, Grant/Award Number: LANCAD-UNAM-DGTIC 250; Dirección General de Asuntos del Personal Académico, Universidad Nacional Autónoma de México, Grant/Award Number: IN205118; Fundación para el Fomento en Asturias de la Investigación Científica Aplicada y la Tecnología, Grant/Award Number: IDI-2018-000177; Ministerio de Ciencia e Innovación, Grant/Award Number: PGC2018-095953- B-I00; European Union, Grant/Award Number: PGC2018-095953-B-I00

Abstract

Hydrogen bonds (HB) are arguably the most important noncovalent interactions in chemistry. We study herein how differences in connectivity alter the strength of HBs within water clusters of different sizes. We used for this purpose the interacting quantum atoms energy partition, which allows for the quantification of HB formation energies within a molecular cluster. We could expand our previously reported hierarchy of HB strength in these systems (*Phys. Chem. Chem. Phys.*, 2016, **18**, 19557) to include tetracoordinated monomers. Surprisingly, the HBs between tetracoordinated water molecules are not the strongest HBs despite the widespread occurrence of these motifs (e.g., in ice I_h). The strongest HBs within H_2O clusters involve tricoordinated monomers. Nonetheless, HB tetracoordination is preferred in large water clusters because (a) it reduces HB anticooperativity associated with double HB donors and acceptors and (b) it results in a larger number of favorable interactions in the system. Finally, we also discuss (a) the importance of exchange-correlation to discriminate among the different examined types of HBs within H_2O clusters, (b) the use of the above-mentioned scale to quickly assess the relative stability of different isomers of a given water cluster, and (c) how the findings of this research can be exploited to indagate about the formation of polymorphs in crystallography. Overall, we expect that this investigation will provide valuable insights into the subtle interplay of tri- and tetracoordination in HB donors and acceptors as well as the ensuing interaction energies within H_2O clusters.

KEYWORDS

coordination number, hydrogen bonding, interacting quantum atoms, water clusters

1 | INTRODUCTION

Hydrogen bonds (HBs) are critical in a wide variety of fields, such as molecular recognition[1] and catalysis.[2] Hence, the understanding of the nature of HBs is an active research avenue in constant development. The correct characterization of HBs is a complicated endeavor whose principal difficulties lie in the description of the nonadditive contributions to these interactions. In other words, the proper account of HBs entails the understanding of how these contacts affect each other increasing (cooperativity) or decreasing (anticooperativity) their formation energies.[3,4]

The study of nonadditivity in water clusters has a lengthy and rich history in experimental and computational physical chemistry. Concerning electronic structure calculations, Clementi and coworkers[5] as

well as Scheiner and Nagle[6] used the supermolecule method among the first efforts to study HBs with quantum chemical methods. These researchers found enhanced dipole moments with respect to that found in an isolated water molecule. Later, more sophisticated investigations which include electronic correlation via the MP2 methodology found a systematic contraction of the O···O separation in adjacent water molecules that takes place from the dimer to the hexamer of water.[7,8] Afterwards, microwave experiments by Saykally et al. confirmed the homodromic cycles within the structures of $(H_2O)_n$ (n = 3–5) and give strong spectroscopic evidence of cooperativity in small water clusters.[9–13] Regarding larger systems, the search for the minimum structures of water clusters via MP2 calculations has continued, for example, with Xantheas who considered recently H_2O clusters with up to 25 monomers.[14] Other authors have also used force field potentials to study different properties of water clusters. Tsai and Jordan, for instance, used the TIP4P potential to optimize the structures of water clusters comprising 8, 12, 16, and 20 molecules almost 30 years ago.[15] Hereof, Peterson et al.[16] addressed translational and rotational dynamics of water molecules with the same force field potential but including up to 45,000 monomers. Recently, broadband rotational spectroscopy on clusters of 9 and 10 water molecules have confirmed the presence of cooperative effects in those systems.[17] HB cooperativity is fundamental not only for the microscopic properties of water cluster but also for the macroscopic features of H_2O. At the beginning of the decade Stokely and coworkers used mean-field calculations and Monte Carlo simulations to show that the inclusion of cooperativity within water clusters was fundamental for the correct thermodynamic description of the bulk.[18]

The presence of cooperative effects for water aggregates was already uncontroversial at the end of the twentieth century.[19–21] In contrast, the situation for the opposite effects, that is, HB anticooperativity, was not well established.[22] Among the accepted ideas on this issue, was a strong relationship between antidromic cycles comprising double proton acceptors and donors with HB anticooperativity.[21–23] However, some of us have recently shown how the occurrence of double HB donors and acceptors can also lead to very strong HB interactions in water clusters.[4] This conclusion was obtained as a result of a hierarchy of HB strength based on the single/double and acceptor/donor character of water molecules within H_2O clusters. Despite its correct account of relative HB formation energies within small water clusters, this scale of HB strength in H_2O adducts is incomplete because it does not include tetracoordinated water motifs, which are important arrangements of H_2O molecules in large water clusters as well as in liquid and solid water.

We intend to contribute further in this direction by examining formation energies within water clusters with tetracoordinated monomers using quantum chemical topology (QCT) tools. QCT comprises a set of methodologies that use the language of dynamical systems to partition and to characterize molecules and molecular complexes via the topological analysis of several scalar fields derived from the electronic wave function.[24,25] The methods in QCT have the attractive feature of being invariant to orbital transformations and they are robust against the change of the level of approximation in electronic structure theory.[26] QCT analyses have been used to investigate a variety of non-covalent interactions such as π–π[27] and σ–σ stacking,[28] chalcogen contacts,[29] or pnicogen bonds.[30–32] Two of the methods within QCT that have been very successful in this regard are (a) the quantum theory of atoms in molecules (QTAIM) based on the topology of the electron density and (b) the interacting quantum atoms (IQA) approach, a rigorous partition of the electronic energy-based solely on the state vector of the system under consideration.[33] Different workers have exploited QTAIM and IQA to study halogen,[34–37] beryllium,[38,39] and tetrel bonding[40] to name a few. Most importantly for this work, the use of QTAIM and IQA has provided valuable insights into the understanding of HBs.[3,4,41–43]

Given the main aim of this investigation, this paper is organized as follows. First, we present the theoretical framework of the methods exploited in this investigation and the associated computational details of our calculations. Later on, we summarize and discuss our principal results. Finally, we enumerate our main conclusions. Briefly, we were able to expand our previously reported scale for the strength of HBs within water clusters[4] with the inclusion of tetracoordinated water molecules. We found that the HB formation energies involving tetracoordinated water monomers do not correspond to the strongest HB arrangement as it could have been anticipated given the predominance of these motifs of water molecules, for example, in ice I_h. We also discuss the preference for H-bonds which involve tetracoordinated monomers despite their smaller formation with respect to other motifs, and how our results provide alternative explanations for H-bond cooperativity and anticooperativity. We also consider perspectives for the exploitation of our results in the assessment of the relative stability of isomers of water clusters and the study of polymorphism in crystallography. Overall, we expect that this contribution provides important insights into the complex relationship between the connectivity of H_2O monomers within a cluster and the formation energies associated with the resulting interactions.

2 | THEORETICAL FRAMEWORK

The foundations of QCT were laid out by the development of the QTAIM by Bader and coworkers.[44] The QTAIM is built on the topological examination of the electron density which leads us to recover key chemical concepts, such as atoms, functional groups and chemical bonding from quantum chemical calculations. Additionally, the QTAIM defines a division of the three-dimensional (3D) space in atomic basins, that is, proper quantum subsystems for which we can compute average values of Dirac observables, such as the atomic energy and different atomic multipole moments.[45] Moreover, the QTAIM also defines the delocalization of the electrons of a basin A into another atom B, an indicator of the degree of covalency between these atoms.[46]

Based on the topological division of the 3D space defined by QTAIM, the IQA methodology[33,47] performs a division of the

electronic energy of a molecule or molecular cluster using the first and second-order density matrices of the investigated system. The IQA methodology can be also employed within the formalism of Kohn–Sham theory,[48,49] despite the lack of second-order densities in DFT. More specifically, the IQA analysis conduces to a dissection of the electronic energy in intra-atomic, E^{A}_{net}, and interatomic, E^{AB}_{int}, components,[33,47]

$$E = \sum_{A} E^{A}_{net} + \frac{1}{2}\sum_{A}\sum_{B\neq A} E^{AB}_{int}, \tag{1}$$

wherein A, B, … are the atomic basins defined by the QTAIM. The intra and interatomic contributions can be further decomposed as

$$E^{A}_{net} = T^{A} + V^{AA}_{ne} + V^{AA}_{ee}, \tag{2}$$

and

$$E^{AB}_{int} = V^{AB}_{nn} + V^{AB}_{ne} + V^{BA}_{ne} + V^{AB}_{ee}, \tag{3}$$

with T^{A} being the kinetic energy of atom A, while V^{AB}_{ne} and V^{AB}_{ee} represent (a) the attraction of the nucleus of atom A with the electrons of basin B and (b) the repulsion of the electrons of the same atoms. Finally, V^{AB}_{nn} denotes the repulsion between the nuclei of atoms A and B.

We can also divide the IQA interaction energy between two atoms into classical (V^{AB}_{cl}) and exchange-correlation (V^{AB}_{xc}) contributions,

$$E^{AB}_{int} = V^{AB}_{cl} + V^{AB}_{xc}. \tag{4}$$

The terms V^{AB}_{cl} and V^{AB}_{xc} are commonly identified with ionic and covalent components of the interaction energy between atoms A and B, respectively. The conceptual framework of IQA enables us to regroup the terms of Equation (1) to express the corresponding values of the net and interaction energies for groups of atoms, $\mathcal{G}$, $\mathcal{H}$, $\mathcal{I}$, … within an electronic system, for example, monomers forming a molecular cluster,

$$E = \sum_{\mathcal{G}} E^{\mathcal{G}}_{net} + \frac{1}{2}\sum_{\mathcal{G}}\sum_{\mathcal{G}\neq\mathcal{H}} E^{\mathcal{G}\mathcal{H}}_{int}, \tag{5}$$

in which

$$E^{\mathcal{G}}_{net} = \sum_{A\in\mathcal{G}} E^{A}_{net} + \frac{1}{2}\sum_{A\in\mathcal{G}}\sum_{\substack{B\in\mathcal{G}\\ B\neq A}} E^{AB}_{int}, \tag{6}$$

and

$$E^{\mathcal{G}\mathcal{H}}_{int} = \sum_{A\in\mathcal{G}}\sum_{B\in\mathcal{H}} E^{AB}_{int}. \tag{7}$$

Finally, it is possible to represent the changes in energy associated with the formation of a molecular cluster, $\mathcal{G} + \mathcal{H} + \mathcal{G} \cdots \mathcal{H} \cdots \mathcal{G}$, as the sum,

$$\Delta E = \sum_{\mathcal{G}} E^{\mathcal{G}}_{def} + \sum_{\mathcal{G}}\sum_{\mathcal{G}>\mathcal{H}} E^{\mathcal{G}\mathcal{H}}_{int}, \tag{8}$$

wherein $E^{\mathcal{G}}_{def}$, denotes the deformation energy of group $\mathcal{G}$, namely the difference in energy between (a) $\mathcal{G}$ within the molecular cluster (computed with Equation (6)) and (b) $\mathcal{G}$ isolated in its equilibrium geometry.[33] We can rewrite Equation (8) as a pairwise sum of interacting monomers[4]

$$\begin{aligned}\Delta E &= \sum_{\mathcal{G}}\sum_{\mathcal{G}>\mathcal{H}}\left(E^{\mathcal{G}\mathcal{H}}_{int} + \left(\frac{E^{\mathcal{G}\mathcal{H}}_{int}}{\sum_{\mathcal{J}\neq\mathcal{G}} E^{\mathcal{J}\mathcal{G}}_{int}}\right)E^{\mathcal{G}}_{def} + \left(\frac{E^{\mathcal{G}\mathcal{H}}_{int}}{\sum_{\mathcal{J}\neq\mathcal{H}} E^{\mathcal{J}\mathcal{H}}_{int}}\right)E^{\mathcal{H}}_{def}\right)\\ &= \sum_{\mathcal{G}}\sum_{\mathcal{G}>\mathcal{H}} E^{\mathcal{G}\mathcal{H}'}_{int}.\end{aligned} \tag{9}$$

in which $E^{\mathcal{G}\mathcal{H}'}_{int}$ includes $E^{\mathcal{G}\mathcal{H}}_{int}$ and a fraction of $E^{\mathcal{G}}_{def}$ and $E^{\mathcal{H}}_{def}$. Finally, it is also possible to partition the energy arising from Equation (9), $E^{\mathcal{G}\mathcal{H}'}_{int}$ into classical and exchange-correlation components,

$$\begin{aligned}\Delta E &= \sum_{\mathcal{G}}\sum_{\mathcal{G}>\mathcal{H}}\left(E^{\mathcal{G}\mathcal{H}}_{xc} + E^{\mathcal{G}\mathcal{H}}_{class}\right)\left(1 + \left(\frac{1}{\sum_{\mathcal{J}\neq\mathcal{G}} E^{\mathcal{J}\mathcal{G}}_{int}}\right)E^{\mathcal{G}}_{def} + \left(\frac{1}{\sum_{\mathcal{J}\neq\mathcal{H}} E^{\mathcal{J}\mathcal{H}}_{int}}\right)E^{\mathcal{H}}_{def}\right)\\ &= \sum_{\mathcal{G}}\sum_{\mathcal{G}>\mathcal{H}}\left(E^{\mathcal{G}\mathcal{H}'}_{xc} + E^{\mathcal{G}\mathcal{H}'}_{cl}\right)\end{aligned} \tag{10}$$

3 | COMPUTATIONAL DETAILS

We optimized the structures of 16 water clusters $(H_2O)_n$ n = 6, …, 17, shown in Figure 1. The starting geometries of the examined systems were taken from the literature[14,50,51] and recomputed with the M06-2X/6-311++G(d,p) approximation.[52,53] Later on, single-point calculations were performed at the M06-2X/aug-cc-pVTZ[54,55] level of theory. All these calculations were carried out using the package GAUSSIAN09.[56] We decided to employ this methodology because the combination of this exchange-correlation functional with basis sets of triple-zeta quality reproduces adequately the cooperative and anticooperative behavior described by correlated wavefunctions at a moderate computational cost.[57] Later on, using the electronic densities computed via DFT we proceeded to analyze the QTAIM topological properties of the electron density and to carry out the IQA energy partition.[48,49] We used the AIMALL program for these purposes.[57] The visualization of our results was carried out with the help of the GAUSSVIEW program[56] and the MATPLOTLIB[58] library.

4 | RESULTS AND DISCUSSION

4.1 | Hierarchy of H-bond strength within water clusters

As stated in Section 1, we had previously suggested a scale for the strength of HBs between water molecules based on the single and double character of the involved hydrogen bond donors and

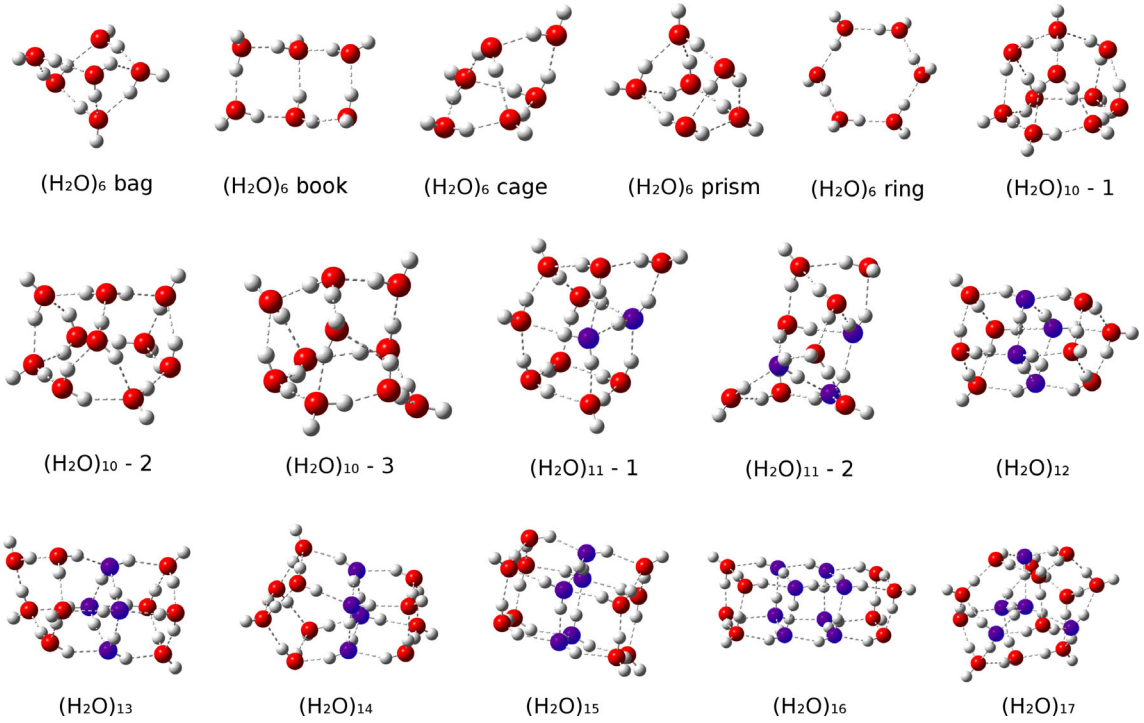

FIGURE 1 Water clusters considered in this work. The oxygen atoms corresponding to tetracoordinated H_2O molecules are highlighted in darker color [Color figure can be viewed at wileyonlinelibrary.com]

acceptors.[4] This scale is incomplete, however, because it does not include tetracoordinated water monomers. By considering the systems shown in Figure 1, we were able to ameliorate this omission. Table 1 describes the 10 categories in which we separated the different types of HBs within the investigated water clusters. This new scale includes the six types of HB considered before[4] as well as four new categories which entail tetracoordinated water molecules. The types of HB in Table 1 are ordered from less (1) to most (10) energetic. The averages of the formation energies between water molecules for the different types of HB are presented in Figure 2.

These values span from 4.9 ± 0.8 to 8.0 ± 0.5 kcal/mol. We recall at this point that the binding energy of the water dimer computed with the approximation used in this work is −5.2 kcal/mol. Thus, hydrogen bond formation energies within water clusters can be reduced by ≈25% (anticooperativity) or increased by ≈65% (cooperativity). Figure 2 also presents the formerly suggested scale in reference [4]. We point out the good agreement between the old and new data, in particular considering that the previous work relied on MP2/aug-cc-pVTZ electronic structure calculations. We note, however, an inversion for the order of the hydrogen bond types (4) and (5) of the previous scale. But, we also point out that the formation energies of these HBs in such a hierarchy are very similar −7.01 and −6.96 kcal/mol.[4] The closeness of both scales is consistent with previous reports which state that the description of HB cooperativity and anticooperativity is robust with respect to changes in different approximations in electronic structure theory.[57]

Figure 2 shows that the interaction between two tetracoordinated H_2O molecules, type number (6), lies in the middle of the scale. Thus, we can say that tetracoordinated water monomers are close to what can be considered the average of the range of hydrogen bond formation energies within water clusters. The arithmetic mean of the computed formation energies is −6.0 kcal/mol and it corresponds to HB (5) −6.0 ± 0.6 kcal/mol while that for two tetracoordinated H_2O monomers is −6.3 ± 0.4 kcal/mol. Other categories that include tetracoordinated water molecules are (2), (3), and (7).

Espinosa et al. suggested to estimate the formation energy corresponding to an HB via the expression[59]

$$E_{HB} \approx 0.5 V(\mathbf{r}_{bcp}), \quad (11)$$

where $\mathbf{r}_{bcp}$ is the position of the bond critical point associated with the HB, and $V(\mathbf{r})$ the potential energy density scalar field. Figure 3 shows the values computed through this formula as well as those from our IQA calculations, $E_{int}^{H_2O\cdots H_2O'}$.

We note that the estimated energy via Equation (11) is in all cases larger than that computed with IQA (formula (9)). These differences become more pronounced as the HB type becomes more energetic. This observation might be related to the results of Mata et al.[60] who investigated the strength of HB interactions under the action of an external electric field ε. The purpose of ε was *to simulate polarization effects on the interaction, for example, those induced by surrounding molecules or ions in solid-state.*[60] As discussed in the next subsection, the scale of Table 1 might be rationalized in terms of charge transfers. Hereof, Ref. [60] indicates that Equation (11) becomes less accurate for larger electric fields, that is, more sizeable charge transfers and

TABLE 1 The scale of hydrogen bond formation energies within water clusters put forward in this investigation

Type of HB	Description
(1)	(a) The H atom involved in the hydrogen bond belongs to a double HB donor and (b) the oxygen that participates in the interaction acts as a double HB acceptor
(2)	A tetracoordinated water molecule either (a) donates an HB to a tricoordinated double HB acceptor or (b) accepts an HB from a tricoordinated double HB donor
(3)	A tetracoordinated water molecule interacts with a monomer which is a single HB donor and a single HB acceptor
(4)	(a) The hydrogen of a double HB donor is bonded to the oxygen of a single HB acceptor or (b) the oxygen of a double acceptor interacts with a hydrogen of a single donor
(5)	A hydrogen bond is formed between two double HB donors or two double HB acceptors
(6)	Both water molecules are tetracoordinated
(7)	A tetracoordinated H_2O molecule either (a) donates an HB to a tricoordinated double HB donor or (b) accepts an HB from a tricoordinated double HB acceptor
(8)	The oxygen of a single HB donor interacts with a hydrogen of a single HB acceptor
(9)	(a) A hydrogen of a double HB acceptor is in contact with the oxygen of a single donor or (b) the O atom of a double donor interacts with a hydrogen of a single acceptor
(10)	The oxygen of a double HB donor interacts with a hydrogen of a double HB acceptor

Note: The hierarchy is presented in increasing order of magnitude of H-bond formation energies.

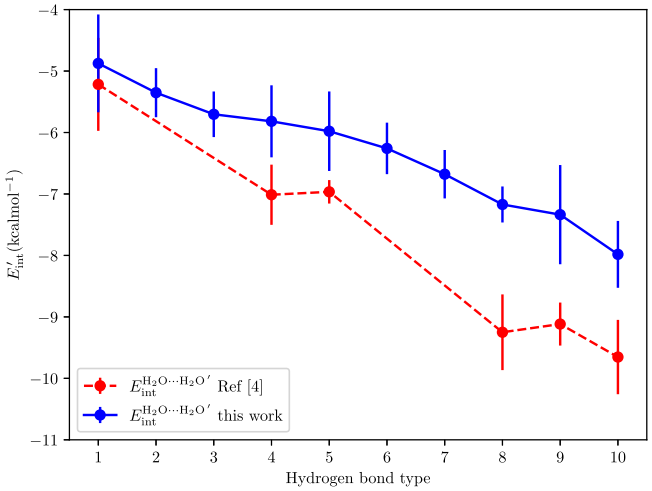

FIGURE 2 Distribution of interacting quantum atoms formation energies, $E^{H_2O\cdots H_2O'}_{int}$ (Equation (9)) between hydrogen-bonded water molecules for the types of hydrogen bonds described in Table 1 [Color figure can be viewed at wileyonlinelibrary.com]

formation energies. However, both ways to calculate the hydrogen bond formation energies (formulae (9) and (11)) agree in the order of the different categories given in Table 1.

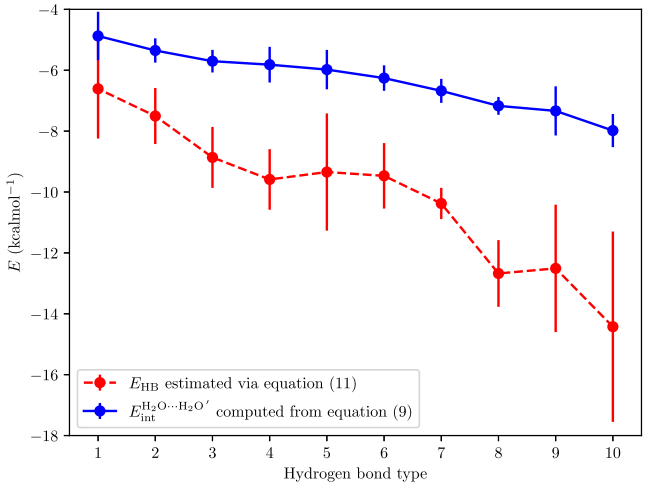

FIGURE 3 Formation energies of the different types of hydrogen bonds specified in Table 1. The values are reported in kcal/mol [Color figure can be viewed at wileyonlinelibrary.com]

4.2 | Charge transfer

The scale of HB strength suggested herein and that put forward in Ref. [4] can be rationalized in terms of the electron charge transfer which occurs in the formation of a hydrogen bond, viz, from the HB acceptor to the HB donor. The left part of the inset in Figure 4a shows a tricoordinated double HB donor for which the electron charge transfer has a twofold effect. First, the two schematized hydrogen bonds in the bottom left part of the inset weaken each other, that is, they present HB anticooperativity. Second, both charge transfers contribute to make the oxygen atom a better HB acceptor, in a similar fashion to the HB donor in $(H_2O)_2$. This effect reinforces the HB in the top left part of Figure 4a. One may consider that double HB donors are relatively poor HB donors but good HB acceptors. Similar arguments based on charge transfers indicate that double HB donors are comparably poor HB donors but good HB acceptors. Because tetracoordinated water molecules are double HB donors and double HB acceptors simultaneously, they are HB donors and acceptors of middle strength. A similar situation occurs for bicoordinated water molecules which are single HB donors and single HB acceptors. We suggest a scale for the HB acceptor and donor capacities within water clusters in Figure 4a. Therefore, the type of H-bond with the smallest formation energy within H_2O clusters, that is, that on the top of Table 1 involves the weakest HB donor (a double HB donor acting as the HB donor) and the weakest HB acceptor (a double HB acceptor functioning as the HB acceptor) as displayed in Figure 4b. On the other hand, the HB with the largest formation energy within a water cluster, viz, the one in the bottom of Table 1 on the scale entails the strongest HB acceptor (a tricoordinated double HB donor operating as the HB acceptor) and the strongest HB donor (a tricoordinated double HB acceptor being the corresponding HB donor) as schematised in Figure 4c. Likewise, the weakest type of HB in which a tetracoordinated water molecule participates (type (2) in Table 1) involves also either a poor HB donor or a poor HB acceptor.

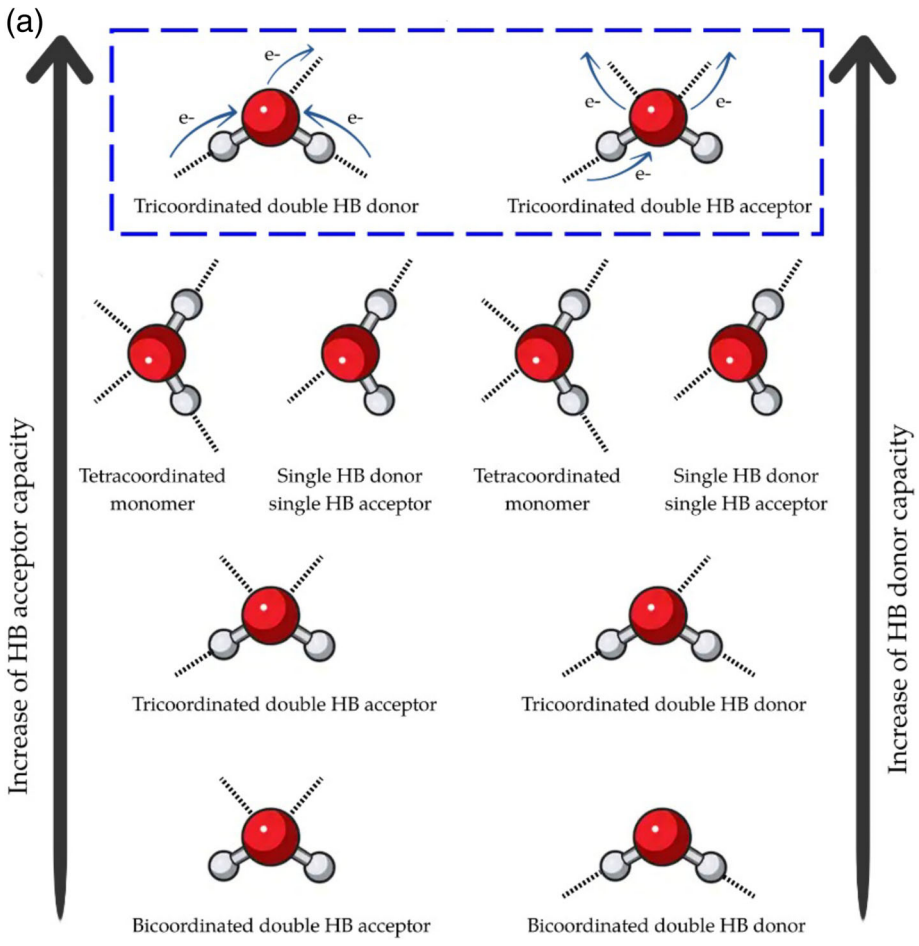

FIGURE 4 (a) Hierarchy of the capacity of H-bond acceptors (left) and donors (rights) based on the electron charge transfer which occurs in the formation of an H-bond schematised in the inset at the top of the figure. (b) and (c) represent the weakest and the strongest interactions within H_2O clusters in the hierarchy of hydrogen bonding strength put forward in this article (Table 1) [Color figure can be viewed at wileyonlinelibrary.com]

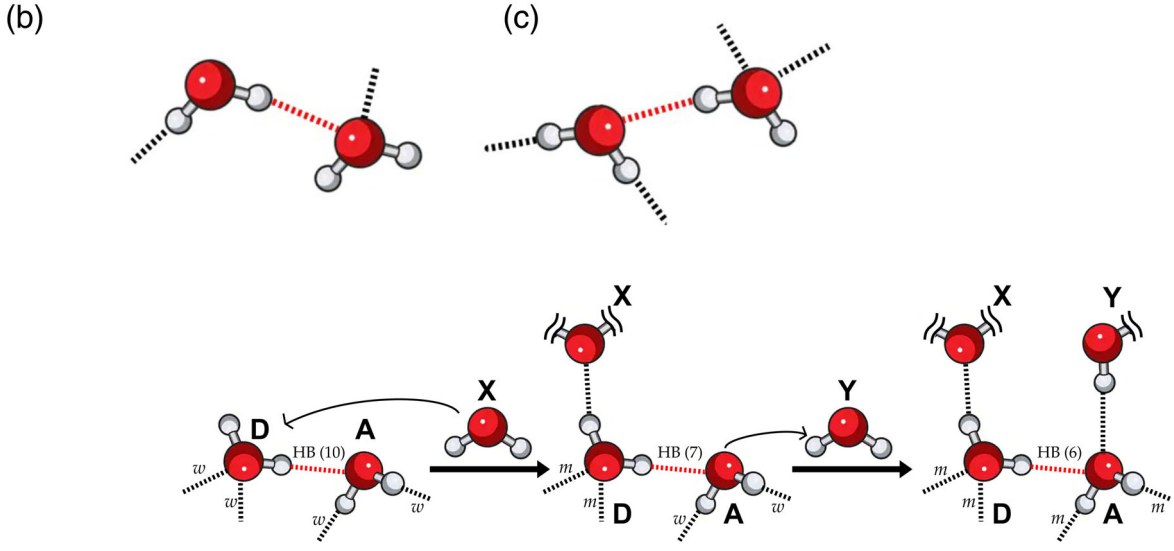

FIGURE 5 Transition from the strongest type of hydrogen bond (HB) in Table 1, namely, HB type (10) (indicated in lighter color) to the interaction between two tetracoordinated molecules (HB kind (6)). The HB sort (7) represents an intermediate stage. While the hydrogen bonding indicated in lighter color is weakened by the formation of the two hydrogen bonds, those labeled with *w* (from "weak") become stronger as indicated with the letter *m* (from "medium force") [Color figure can be viewed at wileyonlinelibrary.com]

Conversely, the HBs with the largest formation energies formed by tetracoordinated H_2O monomers result from their interactions with the strongest HB donors or acceptors (type (7) of HB in Table 1) The kinds of HB (3) and (6) which involve tetracoordinated water molecules as well represent situations that are intermediate between these two extremes.

The transition from the HB in Figure 4c, that is, the strongest of the interactions considered in this investigation, to the HB between two tetracoordinated H_2O monomers as schematised in Figure 5 gives valuable insights on the effects of the formation of tetracoordinated water molecules in H_2O clusters. First, when the HB donor **D** in the left part of Figure 5 becomes a tetracoordinated molecule, it turns into (a) a worse HB donor and (b) a better HB acceptor. The first fact weakens the HB indicated in lighter color in Figure 5, but the second strengthens the two HBs of molecule **D** labeled with the letter *w* in the left part of Figure 5. These enhanced HBs are indicated with the letter *m* in the middle part of the same figure. Likewise, when the fourth HB is formed around molecule **A**, this monomer becomes (a) a worse HB acceptor and (b) a better HB donor. These conditions have similar effects to those just mentioned, that is, the HB indicated in lighter color in Figure 5 is further weakened and the other HBs of **A** becomes stronger. Overall, tetracoordination allows increasing the number of attractive hydrogen bonds within a system while it might strengthen other previously formed HBs. These observations might explain the preponderance of HB tetracoordinated water monomers in large H_2O clusters and in the bulk.[61,62]

The reduction of HB anticooperative effects via the formation of new hydrogen bonds can be illustrated by considering the generation of the prism isomer of the water hexamer from the interaction of two antidromic cycles of $(H_2O)_3$. The top part of Figure 6 shows that the six hydrogen bond formation energies within the antidromic cycles of the H_2O trimers increase in all cases but in one. The magnitudes of the sums of such formation energies rise by 2.29 and 2.78 kcal/mol in the two rings. Also, the hydrogen bond interactions whose formation energy increase as a consequence of the interaction between the two antidromic cycles of $(H_2O)_3$ increase their position (or stay in the same category) in the hierarchy put forward in Table 1. The converse is also

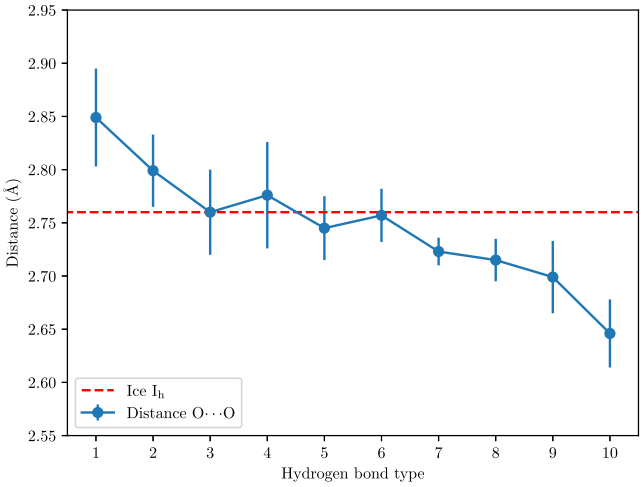

FIGURE 7 Average distances between oxygen atoms for the different H-bond in Table 1. The O···O distance for ice I_h is shown as well. The values are reported in Å [Color figure can be viewed at wileyonlinelibrary.com]

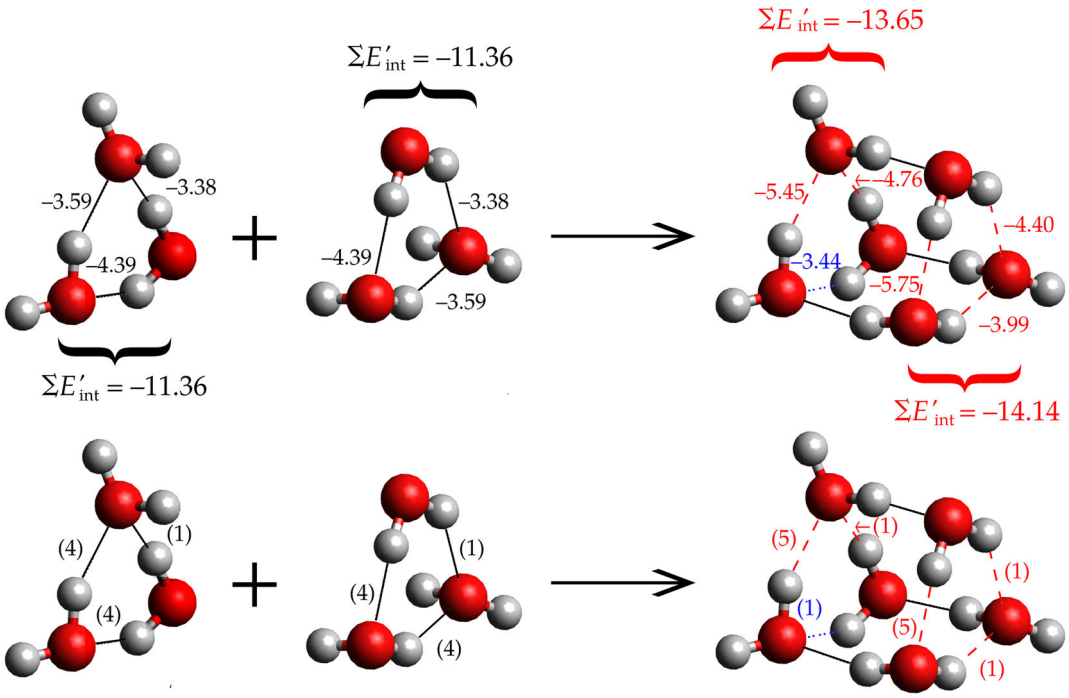

FIGURE 6 Formation of the prism isomer of $(H_2O)_6$ from two interacting antidromic cycles of $(H_2O)_3$. (Top) Formation energies (in kcal/mol) of the hydrogen bonds within the antidromic cycles of $(H_2O)_3$ in isolated form and inside the prism structure of $(H_2O)_6$. The value of the sum of such formation energies for each antidromic cycle of $(H_2O)_3$ is also indicated. (Bottom) Categories within the hydrogen bond strength hierarchy of Table 1. The hydrogen bonds which are strengthened/weakened as a consequence of the interaction of the two H_2O trimers are indicated in dashed/dotted [Color figure can be viewed at wileyonlinelibrary.com]

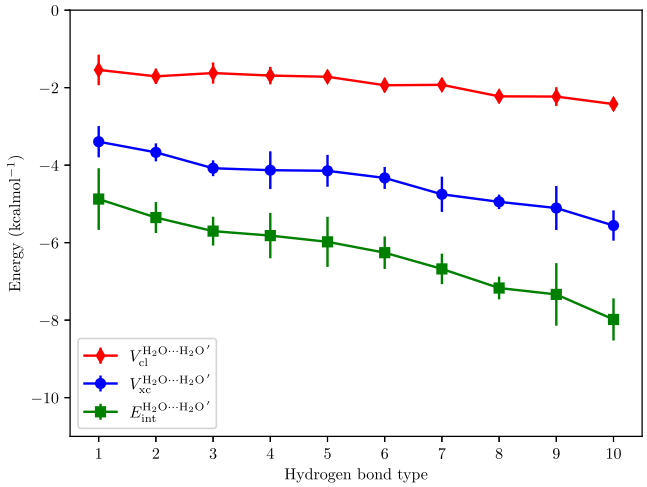

FIGURE 8 Average values for the classical and exchange-correlation contributions to the interaction energy for the different types of hydrogen bonds put forward in Table 1 [Color figure can be viewed at wileyonlinelibrary.com]

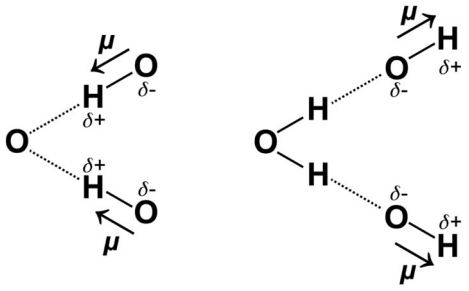

FIGURE 9 Double hydrogen bond acceptor (left) and donor (right). These motifs result in nearly parallel dipoles which are associated with H-bond anticooperativity[21]

true for the HB which reduces its formation energy due to the process illustrated in Figure 6.[2]

4.3 | Relation with ice I_h

Interaction energies and distances between molecules tend to follow similar trends. Figure 7 shows the average distances between oxygen atoms for the different types of HBs in the hierarchy put forward in Table 1. We note that O···O distances follow a similar tendency to those shown in Figures 2 and 3. Namely, longer distances are associated with weaker interactions, while shorter ones are related to stronger contacts, as expected. Figure 7 shows the experimental O···O distance in ice I_h,[63] as well. This value is very similar to the average distance found for the HBs in the middle of the scale, that is, those of the (3)–(6) types. Importantly, type (6) corresponds to the interaction between two tetracoordinated H_2O molecules, which is the bonding situation observed in ice I_h.

Now, we discuss briefly how the formation energy of the hydrogen bonds among tetracoordinated molecules (HB type (6)) can be related to the sublimation energy of ice,

$$H_2O_{(s)} \rightleftharpoons H_2O_{(g)}.$$

The formation energy of HB type (6) is −6.3 kcal/mol. Hence, breaking all of the HBs in ice (composed of tetracoordinated H_2O molecules) would require twice this quantity, that is, −12.6 kcal/mol, an estimation that ignores three and many-body effects. The sublimation enthalpy of ice at 0 K is 11.4 kcal/mol[64] which is in a reasonably good agreement with the estimated value based on the HB formation energies of tetracoordinated molecules. We note at this point that the utilized methodology M06-2X/aug-cc-pVTZ//M06-2X/6-311++G(d,p)

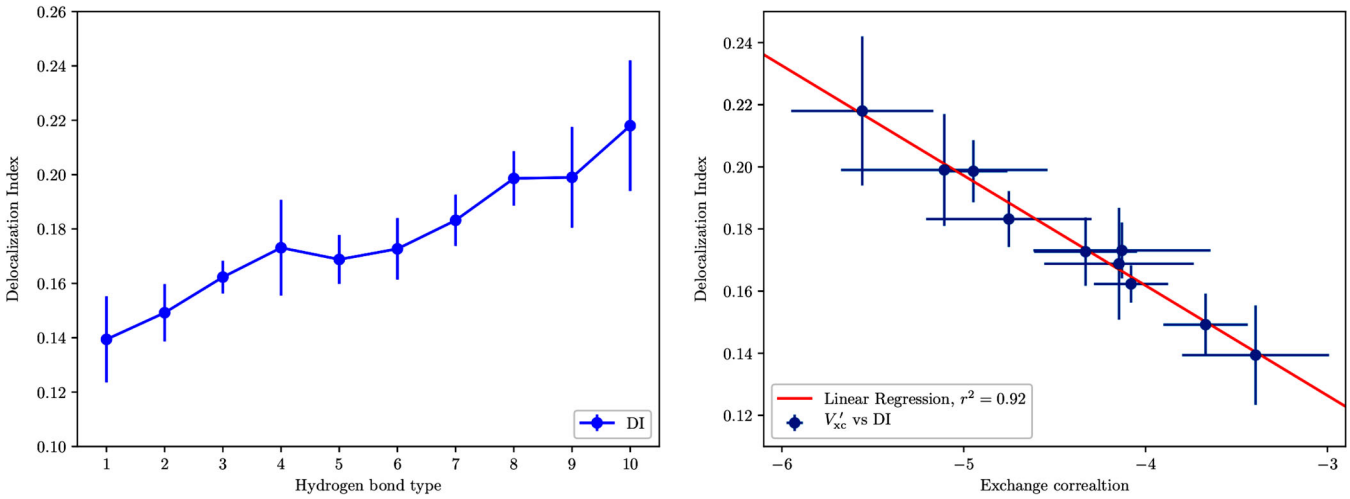

FIGURE 10 Left: Delocalization indices (in a.u.) between hydrogen-bonded water molecules for the different hydrogen bonds shown in Table 1. Right: Correlation between the exchange-correlation contribution to the hydrogen bond formation energy, $V_{xc}^{H_2O\cdots H_2O'}$ (in kcal/mol), and the delocalization indices between hydrogen-bonded water molecules addressed in this investigation [Color figure can be viewed at wileyonlinelibrary.com]

overestimates slightly HB formation energies[65] and hence it also overestimates the sublimation energy of ice I_h at 0 K.

4.3.1 | Covalent vs ionic components of $E_{int}^{H_2O\cdots H_2O'}$

Finally, the IQA energy partition is also able to divide the HB formation energy into classical (ionic) and exchange-correlation (covalent) contributions. Figure 8 shows these contributions to the interaction energy between water molecules for the different types of hydrogen bonds in the scale of Table 1. The values for the classical term, $V_{class}^{H_2O\cdots H_2O'}$, are quite similar for all types of HBs in this hierarchy. On the contrary, the differences for the exchange-correlation term, $V_{xc}^{H_2O\cdots H_2O'}$, are larger. Thus, we can say that the variations in the total interaction energy come mainly from the exchange-correlation part. These observations are in contrast with the above mentioned rationalization of the hierarchy of Table 1 based on arguments of charge transfer and they also disagree with the arguments usually used to

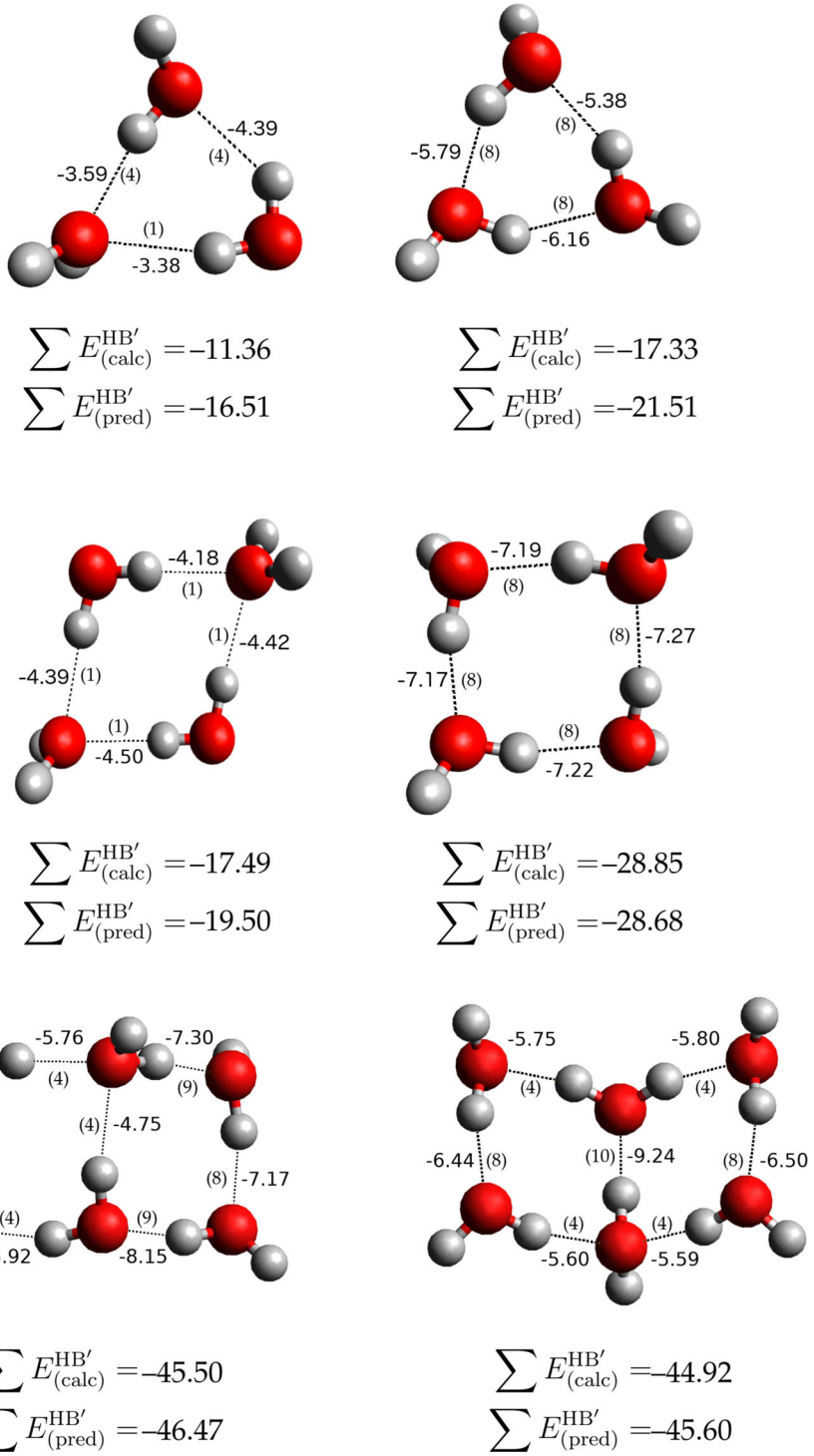

FIGURE 11 Antidromic and homodromic structures of the water trimer (top) and tetramer (middle) as well as two different configurations of the book structure of $(H_2O)_6$. The categories of the hydrogen bonds in Table 1 are shown within parentheses and the hydrogen bond formation energies are calculated with the aid of formula 9. We also report the sum (in kcal/mol) of such computed H-bond formation energies ($\sum E^{HB'}_{(calc)}$) and those predicted with the aid of Table S1 [Color figure can be viewed at wileyonlinelibrary.com]

explain HB anticooperativity.[21] Figure 9 shows a double HB donor and a double HB acceptor which result in the occurrence of nearly parallel dipoles, increasing thereby the energy of the system.[21] We point out in this regard that this explanation is inconsistent with the HB cooperative effects observed between double HB donors and acceptors (Figure 4c) and would result in large differences in $V_{\text{class}}^{H_2O\cdots H_2O'}$ for the different types of H-bonds considered herein as opposed to the results observed in the red curve of Figure 8.

The preponderance of covalency to distinguish among the different types of HBs in Table 1 is also consistent with the quantification of delocalization indices (DIs). The delocalization indices between two atoms (A and B) or groups of atoms ($\mathcal{G}$ and $\mathscr{H}$) indicates the number of electron pairs shared between these moieties.[46,66] The left side of Figure 10 shows the average values for the DIs between water molecules for the different types of HBs addressed in this paper. The hydrogen bonds with the largest formation energies have the most sizeable number of shared pairs of electrons and therefore of covalency as reflected in the values of $DI^{H_2O\cdots H_2O}$ and $V_{xc}^{H_2O\cdots H_2O'}$. There is indeed a strong correlation between these two last-mentioned quantities (right side of Figure 10). Such correlation can be exploited by considering that the computational cost for the calculation of DIs represents only a fraction of that corresponding to $V_{xc}^{H_2O\cdots H_2O'}$.

4.4 | Perspectives

4.4.1 | Energetic assessment of different isomers of water clusters

The scale put forward in Tables 1 and S1 allows for the qualitative and quantitative rationalization for the relative stability of a pair of isomers of a given water cluster. We illustrate this procedure by considering the homodromic and antidromic cycles of $(H_2O)_3$ and $(H_2O)_4$ and two different isomers of the book structure of $(H_2O)_6$ in Figure 11. We note that Table 1 and S1 predict (a) that the antidromic cycles posses H-bonds with lower formation energy than those within the homodromic cycles and (b) that the two considered dispositions of the book configuration of $(H_2O)_6$ are nearly isoenergetic, despite they have different connectivity of H-bonds in their structures. This procedure can be done without performing electronic structure calculations and by simply classifying the HBs within a given water cluster in accordance with Table 1 and by adding the corresponding values of formation energies in Table S1. One can also compute the hydrogen bond formation energies within the examined clusters with the aid of Equation (9). We realize in this way that the hydrogen bonds in the homodromic cycle of $(H_2O)_3$ are 2.00 kcal/mol more stable than in the corresponding antidromic ring. Ditto for $(H_2O)_4$ and 2.84 kcal/mol. Interestingly, the results of Figure 11 reveal that even within antidromic cycles we can have H-bond cooperativity. The hydrogen bonds within the antidromic cycle of $(H_2O)_4$ are stronger than those in the corresponding antidromic cycle of $(H_2O)_3$. We also note that the predictions of $\sum E_{HB}^{H_2O\cdots H_2O}$ via the values reported in Table S1 overestimate considerably those calculated for the trimer due to many-body effects of H-bonding. Nonetheless, the predictions are considerably better for larger clusters as illustrated by the considered structures of $(H_2O)_4$ and examined structures of $(H_2O)_4$ and $(H_2O)_6$. This procedure can be straightforwardly extended to larger clusters and its exploitation warrants a different study in itself.

On polymorph preference in hydrogen-bonded molecular crystals

Our results may also have further implications on the always difficult subject of polymorph preference in hydrogen-bonded molecular crystals, a far-reaching topic in the pharmaceutical industry, for instance.[67] The hierarchy here unveiled signal new possible targets to follow in the growth of molecular clusters toward crystalline nuclei and finally to the solid. We envision a nonnegligible role of the maximization of the number of attractive interactions in such nucleation processes. Mapping a hierarchy landscape similar to the one presented in this work in other systems is thus desirable. If similar conclusions are thereby obtained, one can foresee a more general framework in which the kinetics of nucleation would be determined, or at least influenced, by the growth of those clusters displaying the largest number of "anchoring" points. This groundwork will potentially have a considerable impact on our understanding of the forces driving the formation and observation of polymorphs.

5 | CONCLUDING REMARKS

We have used the IQA energy partition to determine the hydrogen bond formation energies in water clusters which encompass tetracoordinated H_2O monomers. This endeavor allowed us to expand our previously reported classification of hydrogen bonds based on HB connectivity within water hexamers to include tetracoordinated water molecules. The hydrogen bonds which involve tetracoordination are not the strongest interactions considered in this investigation as it could have been expected from the extended occurrence of this HB configuration in nature. Instead, the most marked HB cooperative and anticooperative effects involve tricoordinated water monomers. Nonetheless, tetracoordination is preferred in large H_2O clusters because (a) it reduces HB anticooperative effects which occur due to tricoordinated molecules acting as poor HB donors or acceptors, and (b) it increases the number of attractive interactions within the system. Although the scale of HB strength put forward herein can be rationalized using charge transfer arguments, the covalent character is substantially different among the different types of HBs examined herein, in opposition to the classical arguments based on electrostatics. Finally, we give perspectives for the exploitation of our results for the analysis of the relative stability of isomers of a water cluster and the study of polymorphs in crystallography. Altogether, we expect that the analysis presented herein will prove useful to the understanding of the structure and nature of hydrogen-bonded adducts, for example, water clusters.

ACKNOWLEDGMENTS

We acknowledge financial support from CONACyT/Mexico (grant 253776) and PAPIIT/UNAM (project IN205118). We are also thankful to DGTIC/UNAM for computer time (project LANCAD-UNAM-DGTIC 250). A. M. P. thanks the Spanish MICINN (grant PGC2018-095953-B-I00) the FICyt (grant IDI-2018-000177) and the European Union FEDER funds for financial support.

ORCID

José Manuel Guevara-Vela https://orcid.org/0000-0003-1782-6792
Wilmer E. Vallejo Narváez https://orcid.org/0000-0002-3712-0618
Tomás Rocha-Rinza https://orcid.org/0000-0003-1650-4150

REFERENCES

[1] L. Muñoz-Rugeles, A. Galano, J. R. Alvarez-Idaboy, *Phys. Chem. Chem. Phys.* **2017**, *19*, 15296.
[2] E. Romero-Montalvo, J. M. Guevara-Vela, W. E. Vallejo Narváez, A. Costales, Á. Martn Pendás, M. Hernández-Rodrguez, T. Rocha-Rinza, *Chem. Commun.* **2017**, *53*, 3516.
[3] J. M. Guevara-Vela, R. Chávez-Calvillo, M. Garca-Revilla, J. Hernández-Trujillo, O. Christiansen, E. Francisco, Á. MartnPendás, T. Rocha-Rinza, *Chem. Eur. J.* **2013**, *19*, 14304.
[4] J. M. Guevara-Vela, E. Romero-Montalvo, V. A. Mora Gómez, R. Chávez-Calvillo, M. Garca-Revilla, E. Francisco, Á. Martn Pendás, T. Rocha-Rinza, *Phys. Chem. Chem. Phys.* **2016**, *18*, 19557.
[5] E. Clementi, W. Kolos, G. C. Lie, G. Ranghino, *Int. J. Quantum Chem.* **1980**, *17*, 377.
[6] S. Scheiner, J. F. Nagle, *J. Chem. Phys.* **1983**, *87*, 4267.
[7] S. S. Xantheas, T. H. Dunning, *J. Chem. Phys.* **1993**, *99*, 8774.
[8] S. S. Xantheas, *J. Chem. Phys.* **1994**, *100*, 7523.
[9] M. R. Viant, J. D. Cruzan, D. D. Lucas, M. G. Brown, K. Liu, R. J. Saykally, *J. Phys. Chem. A* **1997**, *101*, 9032.
[10] J. D. Cruzan, M. R. Viant, M. G. Brown, R. J. Saykally, *J. Phys. Chem. A* **1997**, *101*, 9022.
[11] K. Liu, M. G. Brown, J. D. Cruzan, R. J. Saykally, *J. Phys. Chem. A* **1997**, *101*, 9011.
[12] K. Liu, M. G. Brown, R. J. Saykally, *J. Phys. Chem. A* **1997**, *101*, 8995.
[13] K. Nauta, *Science* **2000**, *287*, 293.
[14] A. Rakshit, P. Bandyopadhyay, J. P. Heindel, S. S. Xantheas, *J. Chem. Phys.* **2019**, *151*, 214307.
[15] C. J. Tsai, K. D. Jordan, *J. Phys. Chem.* **1993**, *97*, 5208.
[16] G. Camisasca, N. Galamba, K. T. Wikfeldt, L. G. M. Pettersson, *J. Chem. Phys.* **2019**, *150*, 224507.
[17] C. Pérez, D. P. Zaleski, N. A. Seifert, B. Temelso, G. C. Shields, Z. Kisiel, B. H. Pate, *Angew. Chem. Int. Ed.* **2014**, *53*, 14368.
[18] K. Stokely, M. G. Mazza, H. E. Stanley, G. Franzese, *Proc. Natl. Acad. Sci. U. S. A.* **2010**, *107*, 1301.
[19] J. K. Gregory, *Science* **1997**, *275*, 814.
[20] S. S. Xantheas, *Chem. Phys.* **2000**, *258*, 225.
[21] T. Steiner, *Angew. Chem. Int. Ed.* **2002**, *41*, 48.
[22] M. C. Symons, *J. Mol. Struct.* **1993**, *297*, 133.
[23] W. Saenger, *Nature* **1979**, *279*, 343.
[24] P. L. A. Popelier, *Intermolecular forces and clusters I*, Springer, Berlin, Heidelberg **2005**, p. 1.
[25] P. L. A. Popelier, *Applications of topological methods in molecular chemistry*, Springer International Publishing, Berlin, Heidelberg **2016**.
[26] C. F. Matta, *J. Comput. Chem.* **2010**, *31*, 1297.
[27] C. Trujillo, G. Sánchez-Sanz, *ChemPhysChem* **2015**, *17*, 395.
[28] M. Alonso, T. Woller, F. J. Martn-Martnez, J. Contreras-Garca, P. Geerlings, F. DeProft, *Chem. – Eur. J.* **2014**, *20*, 4931.
[29] G. Sánchez-Sanz, C. Trujillo, I. Alkorta, J. Elguero, *ChemPhysChem* **2012**, *13*, 496.
[30] G. Sánchez-Sanz, C. Trujillo, M. Solimannejad, I. Alkorta, J. Elguero, *Phys. Chem. Chem. Phys.* **2013**, *15*, 14310.
[31] G. Sánchez-Sanz, C. Trujillo, I. Alkorta, J. Elguero, *Phys. Chem. Chem. Phys.* **2014**, *16*, 15900.
[32] G. Sánchez-Sanz, C. Trujillo, *J. Phys. Chem. A* **2018**, *122*, 1369.
[33] M. A. Blanco, A. Martn Pendás, E. Francisco, *J. Chem. Theory Comput.* **2005**, *1*, 1096.
[34] O. A. Syzgantseva, V. Tognetti, L. Joubert, *J. Phys. Chem. A* **2013**, *117*, 8969.
[35] K. Eskandari, M. Lesani, *Chem. – Eur. J.* **2015**, *21*, 4739.
[36] J. M. Guevara-Vela, D. Ochoa-Resendiz, A. Costales, R. Hernández-Lamoneda, Á. Martn Pendás, *ChemPhysChem* **2018**, *19*, 2512.
[37] N. Orangi, K. Eskandari, J. C. R. Thacker, P. L. A. Popelier, *ChemPhysChem* **2019**, *20*, 1922.
[38] K. Eskandari, *Comput. Theor. Chem.* **2016**, *1090*, 74.
[39] J. L. Casals-Sainz, F. Jiménez-Grávalos, A. Costales, E. Francisco, Á. Martn Pendás, *J. Phys. Chem. A* **2018**, *122*, 849.
[40] J. L. Casals-Sainz, A. Costales, E. Francisco, Á. Martn Pendás, *Molecules* **2019**, *24*, 2204.
[41] J. M. Guevara-Vela, E. Romero-Montalvo, A. Costales, Á. Martn Pendás, T. Rocha-Rinza, *Phys. Chem. Chem. Phys.* **2016**, *18*, 26383.
[42] I. Alkorta, I. Mata, E. Molins, E. Espinosa, *Chem. Eur. J.* **2016**, *22*, 9226.
[43] O. J. Backhouse, J. C. R. Thacker, P. L. A. Popelier, *ChemPhysChem* **2019**, *20*, 555.
[44] R. F. W. Bader, *Atoms in Molecules: A Quantum Theory*, Oxford University Press, Oxford **1990**.
[45] R. F. W. Bader, *Chem. Rev.* **1991**, *91*, 893.
[46] X. Fradera, M. A. Austen, R. F. W. Bader, *J. Phys. Chem. A* **1999**, *103*, 304.
[47] E. Francisco, Á. Martn Pendás, M. A. Blanco, *J. Chem. Theory Comput.* **2005**, *2*, 90.
[48] P. Maxwell, Á. Martn Pendás, P. L. A. Popelier, *Phys. Chem. Chem. Phys.* **2016**, *18*, 20986.
[49] E. Francisco, J. L. Casals-Sainz, T. Rocha-Rinza, A. M. Pendás, *Theor. Chem. Acc.* **2016**, *135*, 170.
[50] S. Yoo, E. Aprà, X. C. Zeng, S. S. Xantheas, *J. Phys. Chem. Lett.* **2010**, *1*, 3122.
[51] J. Segarra-Mart, M. Merchán, D. Roca-Sanjuán, *J. Chem. Phys.* **2012**, *136*, 244306.
[52] Y. Zhao, D. G. Truhlar, *J. Phys. Chem. A* **2006**, *110*, 13126.
[53] A. D. McLean, G. S. Chandler, *J. Phys. Chem. A* **1980**, *72*, 5639.
[54] T. H. Dunning, *J. Chem. Phys.* **1989**, *90*, 1007.
[55] R. A. Kendall, T. H. Dunning, R. J. Harrison, *J. Chem. Phys.* **1992**, *96*, 6796.
[56] M. J. Frisch, G. W. Trucks, H. B. Schlegel, G. E. Scuseria, M. A. Robb, J. R. Cheeseman, G. Scalmani, V. Barone, B. Mennucci, G. A. Petersson, H. Nakatsuji, M. Caricato, X. Li, H. P. Hratchian, A. F. Izmaylov, J. Bloino, G. Zheng, J. L. Sonnenberg, M. Hada, M. Ehara, K. Toyota, R. Fukuda, J. Hasegawa, M. Ishida, T. Nakajima, Y. Honda, O. Kitao, H. Nakai, T. Vreven, J. A. Montgomery Jr., J. E. Peralta, F. Ogliaro, M. Bearpark, J. J. Heyd, E. Brothers, K. N. Kudin, V. N. Staroverov, R. Kobayashi, J. Normand, K. Raghavachari, A. Rendell, J. C. Burant, S. S. Iyengar, J. Tomasi, M. Cossi, N. Rega, J. M. Millam, M. Klene, J. E. Knox, J. B. Cross, V. Bakken, C. Adamo, J. Jaramillo, R. Gomperts, R. E. Stratmann, O. Yazyev, A. J. Austin, R. Cammi, C. Pomelli, J. W. Ochterski, R. L. Martin, K. Morokuma, V. G. Zakrzewski, G. A. Voth, P. Salvador, J. J. Dannenberg, S. Dapprich, A. D. Daniels, O. Farkas, J. B. Foresman, J. V. Ortiz, J. Cioslowski, D. J. Fox, *Gaussian 09 Revision D.01*, Gaussian, Wallingford, CT **2009**.
[57] T. A. Keith, *AIMAll (Version 19.02.13)*, TK Gristmill Software, Overland Park, KS **2019** aim.tkgristmill.com.
[58] J. D. Hunter, *Comput. Sci. Eng.* **2007**, *9*, 90.

[59] E. Espinosa, E. Molins, C. Lecomte, *Chem. Phys. Lett.* **1998**, *285*, 170.
[60] I. Mata, I. Alkorta, E. Espinosa, E. Molins, *Chem. Phys. Lett.* **2011**, *507*, 185.
[61] G. Corongiu, E. Clementi, *J. Chem. Phys.* **1993**, *98*, 2241.
[62] S. Kazachenko, A. J. Thakkar, *Mol. Phys.* **2010**, *108*, 2187.
[63] E. M. Schulson, P. Duval, *Creep and fracture of ice*, Cambridge University Press, Cambridge **2009**, p. 5.
[64] R. Feistel, W. Wagner, *Geochim. Cosmochim. Acta* **2007**, *71*, 36.
[65] M. J. Gillan, D. Alfè, A. Michaelides, *J. Chem. Phys.* **2016**, *144*, 130901.
[66] R. F. W. Bader, A. Streitwieser, A. Neuhaus, K. E. Laidig, P. Speers, *J. Am. Chem. Soc.* **1996**, *118*, 4959.
[67] H. G. Brittain, *Polymorphism in Pharmaceutical Solids*, Informa Healthcare, New York **2009**.

SUPPORTING INFORMATION

Additional supporting information may be found online in the Supporting Information section at the end of this article.

How to cite this article: Castor-Villegas VM, Guevara-Vela JM, Vallejo Narváez WE, Martín Pendás Á, Rocha-Rinza T, Fernández-Alarcón A. On the strength of hydrogen bonding within water clusters on the coordination limit. *J Comput Chem*. 2020;1–12. https://doi.org/10.1002/jcc.26391